Pellet-induced MHD activity in H-mode plasmas at ASDEX Upgrade

T. Szepesi[1], G. Cseh[1], L. Horváth[3], G. Kocsis[1], P.T. Lang[2], B. Plöckl[2], G. Pokol[3] and ASDEX Upgrade Team[2]

[1] *Institute for Particle and Nuclear Physics, Wigner Research Centre for Physics, Hungarian Academy of Sciences, EURATOM Association, P.O. box 49, H-1525 Budapest, Hungary*

[2] *Max-Planck-Institut für Plasmaphysik, EURATOM Association, Boltzmannstr. 2, 85748 Garching, Germany*

[3] *Department of Nuclear Techniques, Budapest University of Technology and Economics, Association EURATOM, Műegyetem rkp. 9., H-1111 Budapest, Hungary*

The injection of cryogenic fuelling pellets is foreseen as a powerful tool to manipulate the plasma edge; an important aspect of these, among others, is the triggering of ELMs, and thereby controlling the power output of the plasma. Present experiments at ASDEX Upgrade (AUG) indicate, however, that the pellet-plasma interaction behind ELM triggering is a much more complex process than it was envisaged in the last decade: now, in the full-metal (W) wall tokamak, the type-I ELMy H-mode is much more stable against ELM triggering by pellets, than it has been with the mixed carbon-tungsten wall, where essentially each injected pellet could reliably trigger an ELM [1].

The usual ELM behaviour during pellet injection in the all-metal machine is that the ELM frequency cannot be directly set by the pellet injection frequency; only a fraction of the pellets are able to trigger ELMs, while the rest of them hit already ongoing ELMs or simply burn in the plasma without triggering any instability (like in L-mode). This latter scenario provides the opportunity to study spontaneous and triggered ELMs, as well as undisturbed pellet ablation within the same discharge.

Therefore, the study detailed in [2] was repeated; in [2] the magnetic perturbation driven by the ablating pellet was investigated using a toroidal array of radial pick-up coils [3]. It was found that the pellet drives a high-frequency oscillation in the plasma; to characterise the magnitude of this perturbation, the envelope signal was introduced, which is calculated in the following way: first, a high-pass filter is applied, then the difference of the maximum and minimum of the signal is taken using a box-car. Note that the envelope attained in this way shows very similar behaviour than the integrated power in the 50-300 kHz band ('band power') when calculating the spectrum of the coil signal. Therefore, also in the present study, the envelope is used to characterise the magnitude of the pellet-driven mode.

Besides the magnitude, the spatial properties are also analysed. Using a continuous analytical wavelet transform, the relative phases for all possible pairs of pick-up coils are

calculated on a time-frequency mesh. For a mode having pure sinusoidal structure in the toroidal direction, these relative phases would lie on a straight line as a function of the relative probe position; the slope of the most fitting (in the least squares sense) straight line gives the mode number. According to convention, a negative slope, i.e. a negative mode number indicates a mode rotating towards the ion drift direction, while a mode rotating in the electron drift direction has a positive mode number [4]. Mode numbers are only considered for 'global' modes, meaning that the coherence between all possible pairs of coils signals is at least 0.5.

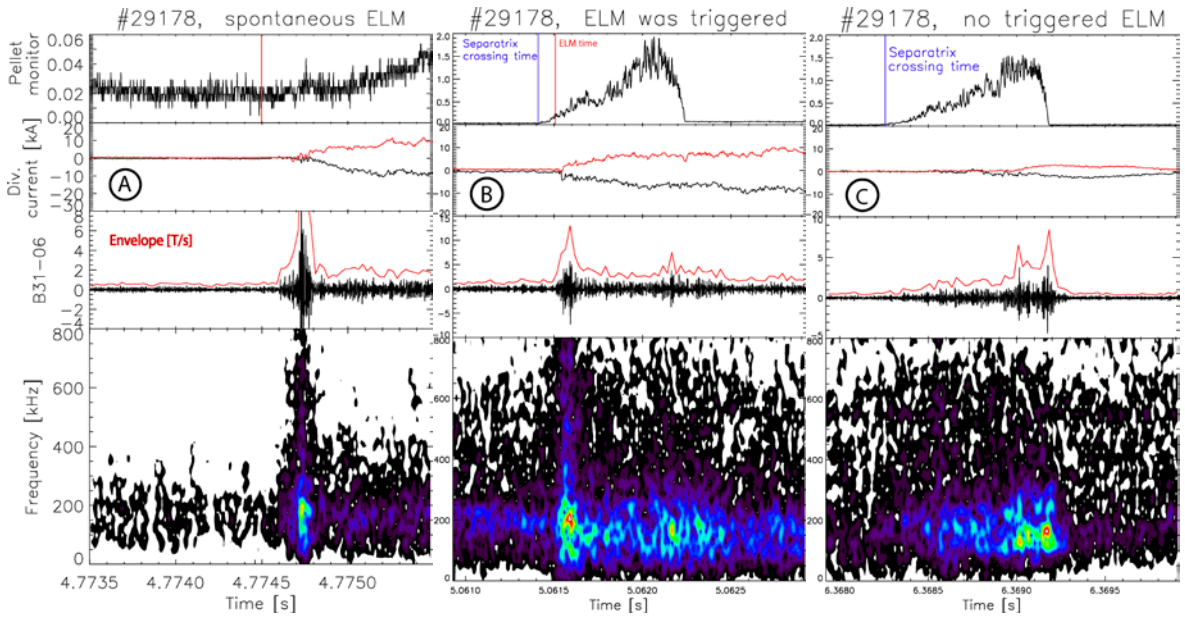

Figure 1: Plasma response to ELM and pellet injection within the same discharge. A spontaneous ELM can clearly be seen on many signals: divertor current, magnetic pick-up coil (marked as B31-06), as well as on the derived envelope and spectrogram (plot A). The pellet triggered ELM shows similar features (plot B), but the presence of the pellet can be seen on both the envelope and spectrogram. These signals exponentially decay after the ablation is over (best seen on plot C). On the right time traces are shown where the pellet cannot trigger an ELM. Note that the divertor current changes only slightly, the envelope features no 'ELM peak' and no activity at high frequencies can be seen on the spectrogram.

Figure 1 shows the plasma behaviour during pellet injection and ELMs. Past experience with the carbon wall tokamak was that only cases shown on plots A and B were detected; with the all-metal wall the third case is also possible. One can easily identify the ELM on all signals for cases A and B: a spike on the envelope, a slower evolving spike on the divertor current and broadband activity on the spectrogram. What we benefit from case C is that there is no triggered ELM, therefore we can directly observe the pellet-driven perturbation, without being masked by the ELM (as in B). It is worth now to re-examine this perturbation magnitude as a function of pellet position in the plasma, as in [2]. The results are shown on Figure 2. It can be seen (plots A and C) that the behaviour of the envelope is very similar in the two cases when there is a triggered ELM: after the ‘ELM-spike’ the envelope is gradually

increasing. However, in the all-metal wall case there are also pellets which do not trigger ELMs, shown in blue on B and separately on D. These traces resemble the L-mode data (shown on C) from the carbon wall machine, proving true the assumption in [2] that the pellet-driven perturbation magnitude is also gradually increasing in H-mode with increasing distance of the pellet from the separatrix.

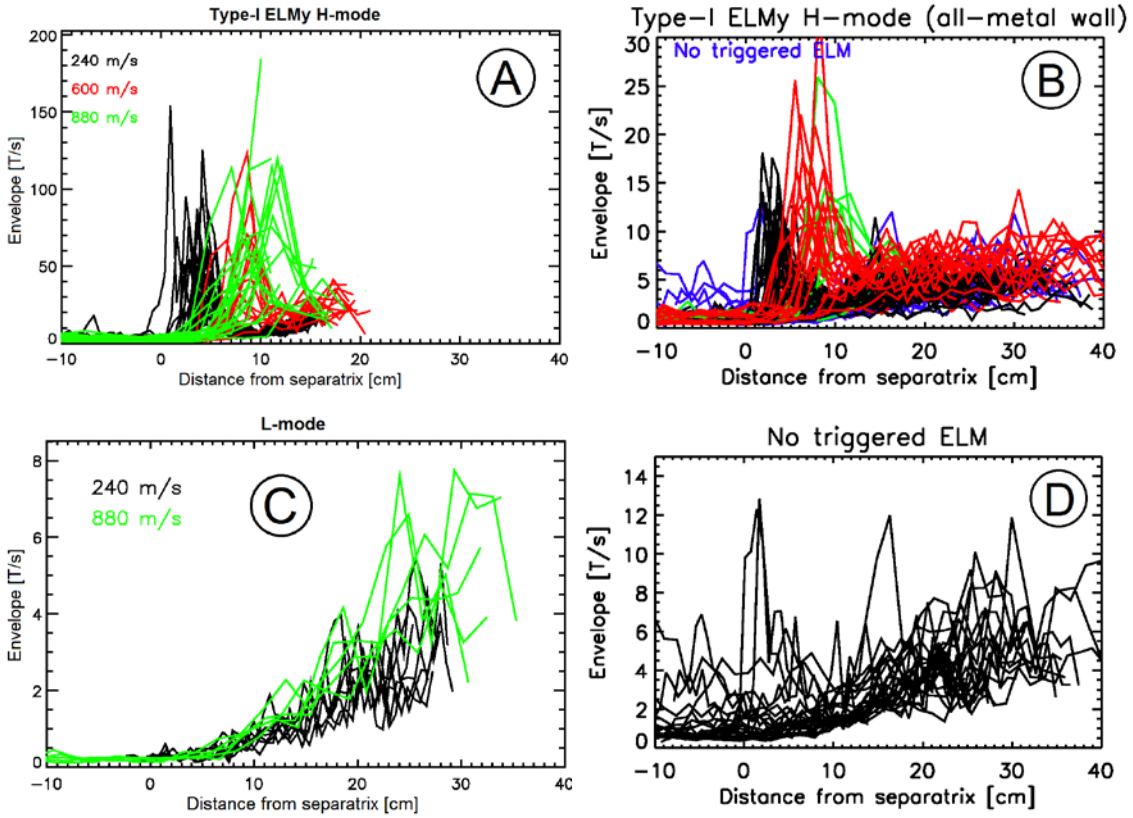

Figure 2: Envelope of the pick-up coil signal as the measure of the pellet-induced magnetic perturbation magnitude. Plots A and C show data from the carbon wall machine, while plots B and D present results from all-metall wall discharges. The different colors denote different pellet velocities (see A and C), valid for all plots. Traces are only shown until the end of pellet ablation, therefore the decay of the signals is not visible.

In order to gain more insight to ELM behaviour in the all-metal wall case, another study was also re-visited, investigating the delay time of pellet triggered ELMs [5]. The ELM delay (dt_{delay}) is the time difference between the pellet crossing the separatrix (determined by video analysis, see P1.146) and the emergence of the ELM on pick-up coil signals. It was assumed that the ELM is always triggered in the same location inside the plasma (location of the 'seed perturbation"), i.e. the pellet has to move to this position in order to trigger the ELM. Therefore, the ELM delay has two components: a time-of-flight term and constant term, the latter being and 'internal' delay time (dt_{int}), which is the time needed for the ELM instability to grow, see eq. 1.

$$dt_{delay} = dt_{\text{int}} + \frac{l}{v_{pellet}} \quad (1)$$

where l is the distance the pellet has to travel inside the plasma to the trigger location, and v_{pellet} is the pellet velocity. The internal delay as well as the trigger location inside the plasma was assumed to be constant and the same for all ELMs. In [5] the internal delay was found to be 50 μs ± 7 μs, while the location of the seed perturbation was 27 mm ± 4 mm. However, the ELM delay is also influenced by the time elapsed after the previous ELM. If this elapsed time is too short, the delay time is considerably increased, as shown in Figure 3A. Therefore, a separate fit was applied to data where the elapsed time was shorter than 10 ms.

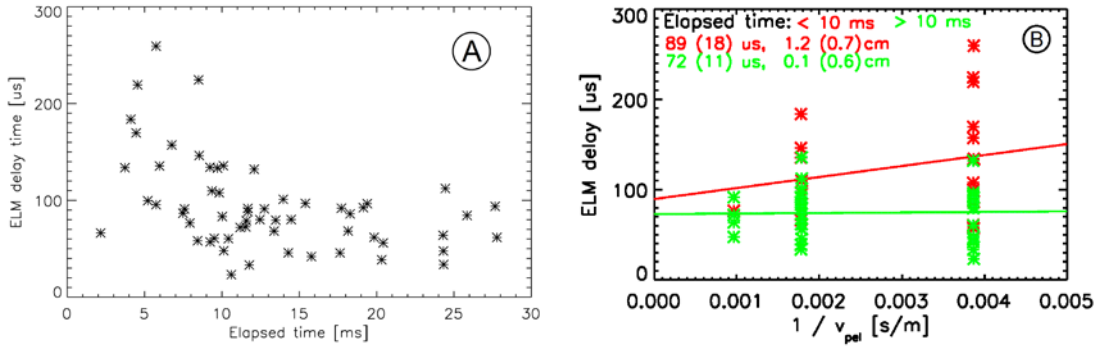

Figure 3: ELM delay time as a function of the elapsed time after the previous ELM (A). Plot B: ELM delay versus 1/v_pellet. Colors denote the two sets of data by elapsed time. Parameters of the fitted lines are also provided with uncertainties: internal delay in μs, and position of the seed perturbation in cm.

Figure 3B reveals that if the elapsed time is too short, the pellet has to travel deeper into the plasma to trigger the ELM. Additionally, these ELMs were also found to be smaller in terms of plasma energy drop than those with larger elapsed times. However, the internal delay is not significantly different within the error bars, implying a similar ELM instability growth rate for all cases. In general, however, the large scatter of the data points, as well as the close-to-zero slope of the fitted line (in case of larger elapsed times) may suggest that the assumption formulated in eq.1 no longer holds.

Concerning mode numbers, a coherent mode is seen during pellet injection in the 100-200 kHz range, with n = 0, sometimes with n = -12 (this uncertainty is the artifact of the torodial coil array, as the coils are located ~60° apart). The same coherent mode is seen for a very short time after spontaneous ELMs, and also in L-mode during pellet injection. Interestingly, this mode looks the same, regardless of pellet position inside the plasma. This feature needs further investigations.

[1] P.T. Lang et al, Nucl. Fusion **44** (2004) 665
[2] T. Szepesi et al, Plasma Phys. Ctrl. Fusion **51** (2009) 125002
[3] T. Bolzonella et al, Plasma Phys. Ctrl. Fusion **46** (2004) A143
[4] G. Pokol et al, AIP Conf. Proc. **993** (2008) 215
[5] G. Kocsis et al, Nucl. Fusion **47** (2007) 1166